7-1-1994

Contrast Enhancement of Medical Images using Multiscale Edge Representation

Jian Lu
University of California, Davis

Dennis M. Healy Jr.
Dartmouth College

John B. Weaver
Dartmouth College

To appear in *Optical Engineering*, Special Issue on Adaptive Wavelet Transforms

Contrast Enhancement of Medical Images Using Multiscale Edge Representation

Jian Lu

Center for Image Processing and Integrated Computing
University of California, Davis, CA 95616
Phone: (916)752-2387 Fax: (916)752-8894
Email: jian@ece.ucdavis.edu

Dennis M. Healy Jr.

Department of Mathematics and Computer Science
Dartmouth College, Hanover, NH 03755
Phone: (603)646-3327 Fax: (603)646-1312
E-mail: healy@curacao.dartmouth.edu

John B. Weaver

Department of Diagnostic Radiology
Dartmouth-Hitchcock Medical Center
Lebanon, NH 03756
Phone: (603)650-5846 Fax: (603)650-8208
E-mail: john.b.weaver@dartmouth.edu

Abstract

Experience suggests the existence of a connection between the contrast of a grayscale image and the gradient magnitude of intensity edges in the neighborhood where the contrast is measured. This observation motivates the development of edge-based contrast enhancement techniques. In this paper, we present a simple and effective method for image contrast enhancement based on the multiscale edge representation of images. The contrast of an image can be enhanced simply by stretching or upscaling the multiscale gradient maxima of the image. This method offers flexibility to selectively enhance features of different sizes and ability to control noise magnification. We present some experimental results from enhancing medical images and discuss the advantages of this wavelet approach over other edge-based techniques.

Keywords:

Contrast enhancement, multiresolution processing, multiscale edges, medical image processing, wavelet transforms.

1 INTRODUCTION

Identifying the edges of low contrast structures is one of the most common tasks performed by those interpreting medical images. Low contrast structures need to be resolved in all kinds of digital medical images; e.g., computed tomography (CT), magnetic resonance (MR), digital mammography, ultrasound, angiography and nuclear medicine. Obtaining high contrast in the raw image directly from the imaging device is almost always expensive in examination time or X-ray dose to the patient. For example, the low contrast in CT is only increased by raising the number of photons absorbed in each voxel, which is proportional to the X-ray dose.[1] So, while most medical images contain important structures having low natural contrast with the surrounding structures, the production of these images generally involves a compromise between the need for enhanced contrast and the various costs of obtaining it. In these situations, digital post processing can play a very important role.

From an image processing point of view, the contrast problem is similar for images obtained from many of the medical imaging modalities described above. In many cases, low contrast can be considered as a result of "bad" distribution of pixel intensities over the dynamic range of the display device. This suggests the application of contrast enhancement methods in an attempt to modify the intensity distribution of the image.

The universally used method of displaying low contrast edges in medical images utilizes linear intensity scaling and clipping; this is commonly called windowing the image because it maps a partial range (window) of the grayscale to the full dynamic range of the display device. Windowing the image brings up the contrast in a certain grayscale window at the expense of saturating pixels which fall outside the window. Since grayscale levels often drift across the image, either prior knowledge or intensive human interaction is needed to choose the right window at each part of the image. The laboriousness of this procedure motivates the search for additional, more automated techniques for increasing the overall contrast in images. Such methods would allow low contrast edges to be identified and followed much more easily.

Windowing itself can be regarded as a method of contrast enhancement. It is a special case of a general technique known as histogram modification.[2] Without prior knowledge about the image to be enhanced, a frequently chosen method is histogram equalization, in which one attempts to make the pixel intensities uniformly distributed over the available dynamic range. However, for images containing large homogeneous regions, such as a flat background, applying histogram equalization is not very effective and in fact serves to magnify noise.

A different approach to contrast enhancement begins with heuristic ideas. It appears that the contrast of a grayscale images correlates highly with the gradient magnitude of intensity edges in the neighborhood where the the contrast is measured. Indeed, any area in an image exhibiting highly visible edges must be of high contrast. This suggests that the contrast of an image can be enhanced by amplifying the magnitude of edge gradients, or the difference of pixel intensities between the both sides of edges. From this perspective it is also evident that contrast enhancement is spatially-dependent. In particular, it seems reasonable that the increase of contrast should be perpendicular to edge contours.

The above observations have led to the development of edge-based contrast enhancement techniques. There are basically two types of such techniques that we know of. In the first type, e.g. in the work of Leu,[3] or in that of Beghdadi and Le Negrate,[4] a pointwise intensity transformation is still used. Edge pixels are identified and used as "indices" in the design of transform functions. A second type of edge-based contrast enhancement has been proposed by Kim and Yaroslavskii,[5] and by Neycenssac.[6] In this approach, filters are applied to the image to amplify the magnitude of edge gradients. In fact, it is identical to the "unsharp masking"[2] used for edge enhancement. A discussion of the limitations of the above two types of techniques is given in Section 5.

In this paper, we propose a new method for contrast enhancement based on a multiscale edge representation originally developed by Mallat and Zhong.[7] Our method is motivated by the fact that the intensities of pixels enclosed within an object boundary can be reconstructed precisely from multiscale edges corresponding to that object. Typically, these pixels vary slowly in intensity across the smooth, homogeneous interior of the object, and

their local variance or contrast need not to be altered. Therefore, we can apply an intensity transformation to multiscale edges only and reconstruct the interior pixels by Mallat and Zhong's algorithm. This has the effect of retaining the homogeneity of intensities within a given region while enhancing the contrast between the different regions. A simple and effective transformation is to stretch or upscale the gradient magnitude of multiscale edges ("edge stretching" for short). When the stretching is applied to edge gradients at only selected scales, features and objects of certain sizes will be enhanced. In this way, noise magnification can be controlled by limiting edge stretching at small scales. Noise magnification can be further reduced by using our previously developed denoising algorithm[8] to prefilter out noisy edges.

A more flexible variant of the algorithm performs image segmentation on the basis of the position and structure of the multiscale edges, so that region-adapted local contrast enhancement may be performed. In this approach, one may employ transformations which vary with both scale and location, utilizing the location and scale information contained in the data of the multiscale edge representation. This permits one to place greater emphasis on features from certain localized regions within the image as well as selectively enhancing objects of a certain size.

This paper is organized as follows: Section 2 briefly reviews the multiscale edge representation of images; Section 3 describes the method for contrast enhancement; Section 4 presents experimental results of enhancing medical images; Section 5 discusses the advantages of the wavelet approach over other edge-based techniques, and directions for future development.

2 THE MULTISCALE EDGE REPRESENTATION OF IMAGES

The multiscale edge representation of signals was first described by Mallat[9] and has evolved in two forms, based on multiscale zero-crossings and multiscale gradient maxima respectively. The latter approach, which is to be used in this paper, was originally developed by Mallat and Zhong,[7] and expanded to a tree-structured representation by Lu *et al.*[10,11] We briefly review the multiscale edge representation for 2-D images. For a more detailed description including background material on wavelet transforms, see References 7,9,and 11.

Many studies of image processing and interpretation utilize the important concept of edge features, which are considered to occur at those positions where the image intensity changes rapidly. Several important edge detection algorithms look for local maxima of the gradient of various smoothed versions of the image. This produces a hierarchy of edge features indexed by the various scales or resolution levels, obtained by smoothing the image to various degrees. In this way, edge features can be classified by their characteristic scale.

Mallat and Zhong formalized and studied this concept of multiscale edge representation with the wavelet transform associated with a particular class of (non-orthogonal) spline wavelets. In their approach, a separable spline scaling function $\phi(x,y)$ plays the role of the smoothing filter, and the corresponding oriented wavelets are given by its partial derivatives:

$$\psi^1(x,y) = \frac{\partial}{\partial x}\phi(x,y) \quad \text{and} \quad \psi^2(x,y) = \frac{\partial}{\partial y}\phi(x,y). \tag{1}$$

The associated 2-D dyadic wavelet transform (WT) of a function $f(x,y) \in L^2(R^2)$ at scale 2^j, at position (x,y), and in orientation k is defined in the usual way:

$$\mathcal{W}^k_{2^j} f\ (x,y) = f * \psi^k_{2^j}\ (x,y), \qquad k = 1,2 \tag{2}$$

with $\psi^k_{2^j}(x,y) = \frac{1}{4^j}\psi^k\left(\frac{x}{2^j}, \frac{y}{2^j}\right)$.

The result is a representation of f as a sequence of vector fields indexed by scale, $\left\{\overrightarrow{\mathcal{W}_{2^j}f}(x,y)\right\}_j$ with:

$$\overrightarrow{\mathcal{W}_{2^j}f}\,(x,y) = \left(\mathcal{W}^1_{2^j}f\,(x,y), \mathcal{W}^2_{2^j}f\,(x,y)\right) \tag{3}$$

An important feature of this representation is the information it provides about the gradient, and hence the edges of f; one may easily show that the 2-D WT defined by (2) gives the gradient of $f(x,y)$ smoothed by $\phi(x,y)$ at dyadic scales. We call this the "multiscale gradient":

$$\begin{aligned} \nabla_{2^j}f(x,y) &\stackrel{\text{def}}{=} \overrightarrow{\mathcal{W}_{2^j}f}\,(x,y) = \left(\mathcal{W}^1_{2^j}f(x,y), \mathcal{W}^2_{2^j}f(x,y)\right) \\ &= \frac{1}{2^{2j}}\nabla(\phi_{2^j} * f)(x,y) \\ &= \frac{1}{2^{2j}}\nabla f * \phi_{2^j}(x,y) \end{aligned} \tag{4}$$

This multiscale gradient representation of f is complete. Indeed, while the wavelets used by Mallat and Zhong are not orthogonal, they do form a nice frame and f may be recovered from $\left\{\overrightarrow{\mathcal{W}_{2^j}f}(x,y)\right\}_j$ through the use of an associated family of synthesis wavelets. Furthermore, these calculations may be done efficiently and stably. In fact, all of the forward and inverse transform computations are actually carried out on discretized data with efficient algorithms utilizing corresponding filters; see the references for details.

When the 2-D function $f(x,y)$ represents the intensity of an image, the positions of rapid variation of f are of interest to us as edge points, and we are led to consider the local maxima of the gradient magnitude at the various scales:

$$\rho_{2^j}f\,(x,y) \stackrel{\text{def}}{=} ||\nabla_{2^j}f(x,y)|| = ||\overrightarrow{\mathcal{W}_{2^j}f}\,(x,y)|| = \sqrt{\left(\mathcal{W}^1_{2^j}f(x,y)\right)^2 + \left(\mathcal{W}^2_{2^j}f(x,y)\right)^2}. \tag{5}$$

More precisely, a point (x,y) is considered a multiscale edge point at scale 2^j if the magnitude of the gradient, $\rho_{2^j}f$, attains a local maximum there along the gradient direction $\theta_{2^j}f$, given by

$$\theta_{2^j}f(x,y) \stackrel{\text{def}}{=} \arctan\left[\frac{\mathcal{W}^2_{2^j}f(x,y)}{\mathcal{W}^1_{2^j}f(x,y)}\right]. \tag{6}$$

For each scale, 2^j, we collect the edge points along with the corresponding values of the gradient (i.e., the wavelet transform values) at that scale. The resulting local gradient maxima set at scale 2^j is then given by,

$$\mathcal{A}_{2^j}(f) = \left\{ [(x_i,y_i); \nabla_{2^j}f\,(x_i,y_i)] \;\middle|\; \begin{array}{l} \rho_{2^j}f(x_i,y_i) \text{ has local maximum at} \\ (x_i,y_i) \text{ along the direction } \theta_{2^j}f(x_i,y_i) \end{array} \right\} \tag{7}$$

For a J-level 2-D WT, the collection

$$\{\mathcal{S}_{2^J} f(x,y), [\mathcal{A}_{2^j}(f)]_{1\le j\le J}\} \tag{8}$$

is called a multiscale edge representation of the image $f(x,y)$. Here $\mathcal{S}_{2^J} f(x,y)$ is the lowpass approximation of $f(x,y)$ at the coarsest scale, 2^J.

An image can be effectively reconstructed from its multiscale edge representation alone. More precisely, we can reconstruct a close approximation of $f(x,y)$ from the data in (8). An algorithm for performing this reconstruction was developed by Mallat and Zhong.[7] It attempts to find a wavelet transform consistent with the sparse data represented by (8) while enforcing a constraint imposed by the reproducing property of wavelet transform; this property is of critical importance to Mallat and Zhong's algorithm. Roughly speaking, the wavelet-transformed images at different scales as defined in (2) are mutually constrained or correlated. The constraint can be expressed in terms of reproducing kernel equations.[12] To enforce such constraint on a set of functions in the reconstruction process, Mallat and Zhong project these functions onto the space characterized by the reproducing kernels.[7] As will be discussed in Section 5, this projection operation is also essential to our technique for reconstructing a contrast-enhanced image.

The multiscale edge representation of images has an immediate application to compact image coding, as was demonstrated by Mallat and Zhong.[13] For sophisticated image analysis and processing tasks, one needs to characterize the structure of the representation set. This is because multiscale edges are not independent primitives and their relationship is invaluable to image analysis. The structure of multiscale edges has been investigated by Mallat and Hwang,[14] and Lu *et al.*[10,11] The work of Mallat and Hwang focused on the characterization of singularities by the Lipschitz regularity which can be measured from the evolution of multiscale edges in scale-space. The work of Lu *et al* led to the construction of a tree-structured multiscale edge representation. Both of these approaches have found applications in image denoising.[8,10,14]

3 CONTRAST ENHANCEMENT BASED ON MULTISCALE EDGES

3.1 The Method

Since the magnitude of edge gradients characterizes the intensity difference between different objects and regions in an image, contrast between objects and regions can be enhanced by applying appropriate transformations on edge gradients. With the multiscale edge representation, different transformations can be designed and used at different scales, thus enabling us to emphasize features of certain sizes. It is also possible to design transformations which place greater emphasis on features from certain spatial regions within the image; this is a simple consequence of the location information contained in the data of the multiscale edge representation.

For a given image f, the simplest transformation on its edge gradients is a linear stretching of the gradient magnitudes. Indeed, for the edge sets $\mathcal{A}_{2^j}(f)$ defined above, we may define the corresponding stretched edge set with stretching factor $k > 1$ simply by multiplying each gradient maximum value by the scalar k :

$$k \cdot \mathcal{A}_{2^j}(f) \stackrel{\text{def}}{=} \left\{ [(x_i,y_i); k\,\nabla_{2^j} f\,(x_i,y_i)] \;\middle|\; [(x_i,y_i); \nabla_{2^j} f\,(x_i,y_i)] \in \mathcal{A}_{2^j}(f) \right\} \tag{9}$$

Notice that this has the effect of scaling the length of the gradient vector at each edge point without affecting its direction.

We may apply these sorts of transformations to each scale in the multiscale edge representation. We distinguish two obvious variations:

Constant Stretching. The stretching is constant at all scales and features of all sizes will be equally enhanced. The transformed multiscale edge set is,

$$\{k \cdot \mathcal{A}_{2^j}\}_j, \qquad k \geq 1 \text{ and independent of scale index } j. \tag{10}$$

Scale Variable Stretching. The stretching is variable depending on scales and features of different sizes will be selectively enhanced. The transformed multiscale edge set is

$$\{k_j \cdot \mathcal{A}_{2^j}\}_j, \qquad k_j \geq 1, \text{ a given function of the scale index } j. \tag{11}$$

In both cases above, a contrast-enhanced image can be reconstructed in two steps. First, the wavelet transform of the enhanced image is reconstructed from the transformed multiscale edge representation by an alternating projection algorithm designed by Mallat and Zhong.[7] Second, an inverse wavelet transform is computed to obtain the enhanced image. There are a couple of modifications we made to Mallat and Zhong's original algorithm in the first step. We start with a modification of the multiscale edge representation of (8), in which the $[\mathcal{A}_{2^j}(f)]_j$ are replaced by (10) or (11). In the iteration of alternating projections, we allow $\mathcal{S}_{2^J} f(x, y)$ to be updated with iterations. In such a way, the reconstruction process not only reconstructs interior pixels between edges, but also alters $\mathcal{S}_{2^J} f(x, y)$ to make it consistent with modified multiscale edges. This ensures that, in addition to enhancing the edges, the contrast between objects and regions separated by edges is enhanced correspondingly.

Let us now examine the effect of multiscale edge stretching with a simple example. Fig. 1(a) is a synthesized low-contrast image of a cube posed in a noisy background. The histogram of this image is shown in Fig. 2(a). Enhanced images shown in Figs. 1(b-d) are obtained by histogram equalization, constant multiscale edge stretching, and scale variable edge stretching, respectively. The histograms corresponding to enhanced images are show in Figs. 2(b-d). It can be observed that histogram equalization magnifies noise drastically by spreading most widely the highest peak (corresponding to the image background) in the histogram. Ideally, we would like to minimize the spread in width of the individual peaks in the histogram, while pulling the peak center positions apart so that the contrast between the image background and three surfaces of the cube will be enhanced. Constant multiscale edge stretching does much better than histogram equalization in this case. It appears that widths of the individual peaks and distances between peaks in the histogram are evenly spread. In the histogram corresponding to scale variable edge stretching, the spread of peak width is further reduced by using a small stretching factor at the finest scale, thus further reducing noise magnification. In Section 4, we will present a case in which we run a denoising algorithm before stretching multiscale edges.

3.2 The Algorithm

We give below an outline of computational steps for image contrast enhancement using the multiscale edge representation. It summarizes the presentation made in Sections 2 and 3.1. To help visualize the algorithm, we have taken a line profile (Row #128) from the cube image in Fig. 1, and have plotted the corresponding profile after each step of the algorithm in Figs. 3-6.

1. The multiscale gradients of a low-contrast image are computed through a wavelet transform using a wavelet of edge detector type (see Fig. 3). For the choice of wavelet edge detectors, see the work of Zhong.[15]

2. Local gradient maxima are detected at all scales and collected in a representation set containing the position, magnitude, and phase angle of all local gradient maxima, and the lowpass approximation of the image at the coarsest scale up to which the wavelet transform is computed (see Fig. 4).

3. The magnitude of gradient maxima is stretched by a constant or by a factor variable at different scales. Replace all gradient maxima in the representation set with modified magnitude values (see Fig. 5).

4. The wavelet transform of the enhanced image is reconstructed from the modified edge representation set by Mallat and Zhong's algorithm. The modified gradient maxima (including their position, magnitude, and phase angle) are strictly retained while the rest of the wavelet transform, including the coarse scale data, is updated with iterative projections (see Fig. 6).

5. The inverse wavelet transform is computed to obtain the contrast-enhanced image (see Fig. 6).

6. If the enhanced image is out of the dynamic range of the display device, rescale it properly and quantize. Clipping may be used in rescaling the image at the expense of saturating pixels at low and high ends of the intensity scale.

In our implementation, we used the cubic spline wavelet among the family of wavelet edge detectors designed by Mallat and Zhong.[7,15] We computed wavelet transforms up to 6 dyadic scales for images of size 256×256 or 512×512. In the reconstruction process, we set 10 to be the maximum number of iterations. In the case where the reconstructed image is out of the dynamic range of the display device, we used clipping with linear scaling to map the image to the available dynamic range.

4 EXPERIMENTAL RESULTS

We now present some experimental results obtained by applying the proposed method to the enhancement of three medical images of different types: mammography, CT, and MR. In the first two cases, results were obtained by using (10) and (11) with or without prefiltering by the denoising algorithm. In the last case, we experimented with a variation of simple edge stretching by making it dependent on the gradient magnitude of multiscale edges.

The contrast in X-ray mammograms is limited by the X-ray dose and the presence of X-ray scatter from dense regions in the breast. Fig. 7(a) is a 256×256 image cropped from a digitized X-ray mammogram. This portion of the mammogram contains a low-contrast mass which might be malignant. Other regions of interest include a cluster of micro-calcifications. Fig. 7(b) is the enhanced image with a constant edge stretching (k=5) at 5 scales. It looks much sharper than the original. Fig. 7(c) is a result of scale variable edge stretching. In this case, the stretching factor decreases linearly as scale increases in order to emphasize features of small sizes. Fine details are highly visible in this enhanced image. Fig. 7(d) is another result of scale variable stretching with emphasis on mid-size features. Note that the suspicious mass and shape of the micro-calcification cluster are clearly brought up.

The contrast in MR is dominated by the relaxation times of the tissues imaged. Increasing the detectability of low contrast structures requires extra scanning time or reduced spatial resolution. Fig. 8(a) is a 256×256 MR image of a human head. With constant multiscale edge stretching at 5 scales, image contrast is improved but noise also becomes quite visible. This enhanced image is shown in Fig. 8(b). To suppress noise magnification with scale variable stretching, we applied a small stretching factor at the finest scale; the result is shown in Fig. 8(c). In this case, noise was not filtered out as much as desired. Therefore, we ran the denoising algorithm before stretching multiscale edges to filter out noisy ones. This denoising algorithm is detailed elsewhere.[8,10] The enhanced image with denoising algorithm and constant multiscale stretching is shown in Fig. 8(d).

Contrast between soft tissue structures in X-ray CT is notoriously small; it is largely determined by the electron density which is almost constant in all soft tissues. Increasing contrast requires increasing the X-ray dose

to the patient. Fig. 9(a) is a typical CT image of brain. One important task here is to identify the boundary between gray matter and white matter, which is very low contrast in CT.[16] The boundary is used to estimate the sizes and volumes of structures in cognitive neuroscience. This image posed a challenge to the method based on simple edge stretching. Fig. 9(b) is the best result we obtained with (9). Using (10) produced similar results. The inadequacy of simple edge stretching for this CT image is due to large separation between peaks in a bimodal distribution of edge gradients. The peak in the low gradient range is contributed mostly by the brain tissue, while the other peak in the high gradient range corresponds to the boundary of the high-contrast skull. The abundance of high-gradient boundaries and the limited dynamic range of display device prevented us from enhancing the brain tissue details characterized by small gradients. We experimented with a variation of simple edge stretching: the stretching factor was made inversely proportional to the magnitude of edge gradients. The results are shown in Fig. 9(c) and 9(d). These two images are different only in the way of requantization; i.e., without and with clipping, respectively (see Section 3.2). The one with clipping gains higher contrast in the brain at the expense of saturating pixels at the high and low ends of the grayscale. However, the overall appearance of both Figs. 9(c) and 9(d) is much better than that can be obtained by grayscale windowing.

5 DISCUSSION

Our experimental results in the previous section suggest that the proposed method for image contrast enhancement is very effective. It is also very simple for images represented by multiscale edges. In this section, we would like to compare our method to other edge-based contrast enhancement techniques, and give some indications of further development.

5.1 A Comparison with Other Edge-Based Techniques

As we reviewed in Section 1, the idea of using edges for image contrast enhancement is not completely new. However, we feel that none of the previously developed techniques exploited the value of edges fully and efficiently.

Leu[3] was motivated to enhance the contrast by increasing the intensity difference between neighboring regions of nearly constant intensity. He derived a histogram equalization function from pixels on edge contours, and applied the same transformation to the entire image. (The actual computation was slightly modified to minimize the number of one-to-many mappings). Recall that we have found that contrast increase must be perpendicular to edge contours. Leu's approach seems a bit indirect and sub-optimal because the histogram does not provide good spatial localization of edges. It would be better to directly work on edges than on their histogram.

The technique of Beghdadi and Le Negrate[4] was built upon the spatial localization of edges. They identified edge contours and used them as indices in the design of intensity transform functions. Using these transform functions, pixel intensities on the different sides of an edge contour were either increased or decreased depending on if they are greater or smaller than the average pixel intensity on the edge contour. A question arises when one tries to implement such a technique: In what range on either side of the edge contour should one apply a certain transform function? There is no simple answer to this question. In their implementation, Beghdadi and Le Negrate used a window. The center of the window was placed at the pixel whose intensity is to be transformed. A single edge contour was estimated inside the window. Then the pixel intensity was compared to the intensity of the edge contour, and was then increased or decreased. The choice of a window size is not easy. In our opinion, there is no "right" size at all in some circumstances. For example, the cube image in Fig. 1 has three visible surfaces, each bounded by four segments of edge contours which separate one surface from the other two and from the background. By Beghdadi and Le Negrate's technique, on each surface one will have different transform functions for pixels close to the different edges. The consequence is that each surface can not be uniformly enhanced and will thus appear distorted. It is not clear to us how to solve this problem completely simply by using a good window.

The approach of Kim and Yaroslavskii,[5] and of Neycenssac[6] is similar to an "unsharp masking" used in edge enhancement. The principle of unsharp masking is well understood (See, e.g. P. 249 in Jain[2]). Fig. 10 shows a profile of a smoothed step edge before and after unsharp masking. One can see immediately a deficiency of this operation when it is used for contrast enhancement. Unsharp masking increases only *locally* the intensity difference between both sides of the edge. If we consider that the step edge in Fig. 10 separates two homogeneous regions, the contrast between them is not enhanced, but the edge is. In practice, when an image contains densely located edges and regions separated by edges are small in support, unsharp masking will make a perceived image of higher contrast. In a more general situation, as in the case of Fig. 10, we need to extend the increased/decreased intensities beyond the small neighborhood of the edge.

By using the multiscale edge representation, we find that we are able to meet these difficulties with some success. To enhance image contrast, we amplify the gradient magnitude of multiscale edges while leaving their phase angles unchanged. This will ensure that the contrast increase is perpendicular to edge contours. There is no need to decide how far away from the edge should one increase or decrease the pixel intensities; the reconstruction process will take care of it. All interior pixels in a region are determined from edges bounding the region, in a manner reminiscent of the solution of a boundary-value problem. In light of this, it is possible to see one difficulty that Beghdadi and Le Negrate's technique is facing: one can not reconstruct the interior pixels from only a segment of the region boundary and expect the reconstructed pixels to be consistent with the full boundary.

The reconstruction process also eliminates the deficiency of unsharp masking for contrast enhancement. Here the projection by the wavelet reproducing kernels plays a critical role. This operation propagates the high values of the amplified edge gradients properly to the interior of a region and enforces consistency of data at all scales.

It appears that some of the difficulties encountered by other edge-based techniques can be handled efficiently and adaptively by using a multiscale edge representation. Additionally, working on multiple scales gives us flexibility to selectively enhance features of different sizes and ability to control noise magnification. There are still potentials that we can explore with a multiscale edge representation.

5.2 Directions for Further Development

The enhancement of the CT image in Section 4 suggested that our technique can be made more adaptive and effective by designing a generalized transformation that is a function of both scale and gradient magnitude of edges. Such a function will be useful for other purposes. For example, when we employ a small stretching factor at fine scales, noise magnification is reduced as noise is often concentrated at small scales. However, this may distort the high frequency components of major edges. As a consequence, the image may become a little blurred. Of course, we could run a separate edge-preserving denoising algorithm as we did in the experiment. However, it is also possible to solve the blurring problem by designing a gradient-dependent transformation.

Research in human visual perception reveals that the contrast sensitivity of the human visual system to visual stimuli obeys Weber's law[17] for a wide range of intensities. If we denote the grayscale intensity by f, then according to Weber's law, a uniform change in intensity, Δf, does not produce uniform change in perception. Rather, the relative change, $\Delta f/f$, is perceived as uniform change in intensity. This implies that the gradient magnitude at an edge alone does not reflect accurately the visual contrast. If an edge gradient is scaled by the magnitude of the edge pixel, it will be a closer measure of contrast. It is clear that by stretching multiscale edges with (10) or (11), the contrast is not uniformly enhanced for dark and bright areas in the image. To uniformly enhance the contrast for all intensity values, we can first take a logarithmic operation on the input image, and then use our technique as described. Finally, we need an exponential operation to get the enhanced image.

A natural development of the methods presented here involves transformations of the multiscale edge representations which vary in space as well as in scale. That is, we consider transformations of the form

$$[(x_i, y_i);\, \nabla_{2^j} f\,(x_i, y_i)] \mapsto [(x_i, y_i);\, k_j(x_i, y_i)\, \nabla_{2^j} f\,(x_i, y_i)]$$

for each edge point (x_i, y_i) in the edge sets $\mathcal{A}_{2^j}(f)$. We are studying an adaptive approach to the construction of the scaling functions $k_j(x_i, y_i)$. This begins with segmentation of the image domain into various subregions of interest, on the basis of the original edge set structure. The edges are grouped into the various subregions, enhanced appropriately, and then the reconstruction is performed.

Before closing the discussion, we would like to point out that similar contrast enhancement results may be obtained in the isotropic stretching cases (constant and scale variable) by stretching all multiscale gradients, i.e., all the wavelet transform coefficients. In this way, the multiscale gradients need not to be reconstructed from their local maxima. However, in order to avoid the undesired phenomenon in unsharp masking (Fig. 10), we would still have to run the iterative reconstruction process to make $S_{2^J} f$ consistent with scaled multiscale gradients.

We generally choose to work with the multiscale edge representation because it provides us with more flexibility. For example, denoising is performed simply in multiscale edge representation by trimming off a number of gradient maxima. Furthermore, in the case of anisotropic stretching, one segments the image into subregions using the edges and then scales the edges according to the subregion to which they belong. It is simplest to then allow the reconstruction algorithm to determine the scaling of the non-edge portions.

6 CONCLUSION

We have presented a description of an edge-based contrast enhancement method, and demonstrated its use with images drawn from three important medical imaging modalities.

Edge-based enhancement offers certain attractive advantages over histogram-based techniques. For example, we want contrast enhancement to take place along the direction perpendicular to edges in the image, and histogram-based techniques do not provide such spatial and orientation localization.

The concept of edge-based contrast enhancement is not completely new; however, previously developed techniques all experience certain difficulties in implementing the basic idea. We have presented some evidence that many of these difficulties can be addressed in an effective way by using a wavelet based multiscale edge representation of images. Additionally, the wavelet approach offers, among other advantages to be further explored, flexibility to selectively enhance features of different sizes and in different locations, as well as the ability to control noise magnification.

7 ACKNOWLEDGMENT

This work was supported in part by ARPA grant DOD F4960-93-1-0567 and a contract from the Naval Surface Warfare Center. Figure 7(a) was provided by the H. Lee Moffitt Cancer and Research Center, USF, Tampa, FL 33612.

8 REFERENCES

[1] H.H. Barrett and W. Swindell, *Radiological Imaging*, Academic Press, New York, 1981, pp. 410-414.

[2] A.K. Jain, *Fundamentals of Digital Image Processing*, Prentice-Hall, Englewood Cliffs, NJ, 1989.

[3] J.-G. Leu, "Image contrast enhancement based on the intensities of edge pixels," *CVGIP: Graphical Models and Image Processing*, Vol. 54, No. 6, pp. 497-506, 1992.

[4] A. Beghdadi and A. Le Negrate, "Contrast enhancement technique based on local detection of edges," *Computer Vision, Graphics, and Image Processing*, Vol. 46, pp. 162-174, 1989.

[5] V. Kim and L. Yaroslavskii, "Rank algorithms for picture processing," *Computer Vision, Graphics, and Image Processing*, Vol. 35, pp. 234-259, 1986.

[6] F. Neycenssac, "Contrast enhancement using the Laplacian-of-a-Gaussian filter," *CVGIP: Graphical Models and Image Processing*, Vol. 55, No. 6, pp. 447-463, 1993.

[7] S.G. Mallat and S. Zhong, "Characterization of signals from multiscale edges," *IEEE Trans. Pattern Anal. and Machine Intell.*, vol. PAMI-14, pp. 710-732, July 1992.

[8] J. Lu, J.B. Weaver and D.M. Healy, Jr., "Noise reduction with multiscale edge representation and perceptual criteria," in *Proc. of IEEE-SP Intl. Symp. on Time-Frequency and Time-Scale Analysis*, Victoria, BC, Oct. 1992, pp. 555-558.

[9] S.G. Mallat, "Zero-crossings of a wavelet transform," *IEEE Trans. Inform. Theory*, vol. IT-37, pp. 1019-1033, July 1991.

[10] J. Lu, "Signal recovery and noise reduction with wavelets," Ph.D. Dissertation, Dartmouth College, Hanover, NH, 1993.

[11] J. Lu, D.M. Healy, Jr. and J.B. Weaver, "A tree-structured multiscale edge representation and applications," in preparation.

[12] A. Grossmann and J. Morlet, "Decomposition of Hardy functions into square integrable wavelets of constant shape," *SIAM J. Math.*, Vol. 15, pp. 723-736, 1984.

[13] S.G. Mallat and S. Zhong, "Compact image coding from multiscale edges," in *Proc. Intl. Conf. Acoust. Speech and Signal Proc.*, Toronto, May 1991.

[14] S.G. Mallat and W.-L. Hwang, "Singularity detection and processing with wavelets," *IEEE Trans. Inform. Theory*, Vol. 38 No. 2, pp. 617-643, March 1992.

[15] S. Zhong, "Signal representation from wavelet transform maxima," Ph.D. Dissertation, New York University, 1990.

[16] R.A. Brooks, G. DiChiro and M.R. Keller, "Explanation of cerebral white-gray contrast in computed tomography," *Journal of Computer Assisted Tomography*, Vol. 4, No. 4, pp. 489-491.

[17] T.N. Cornsweet, *Visual Perception*, Academic Press, New York, 1970.

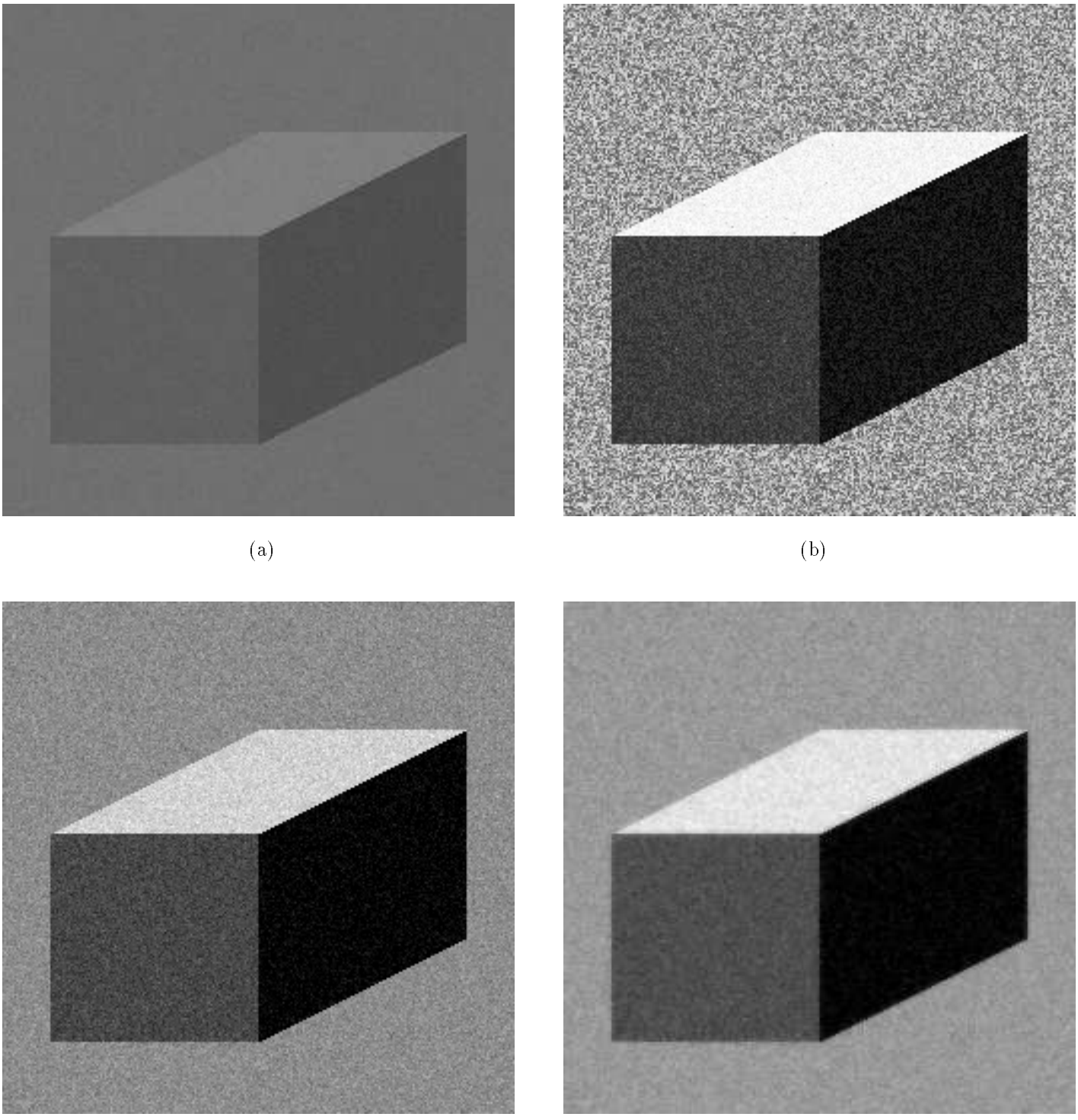

(a) (b)

(c) (d)

Figure 1: Enhancement of a simulated image. (a) A synthesized low-contrast image of a cube posed in a noisy background; (b) enhanced by histogram equalization; (c) enhanced by constant multiscale edge stretching at 6 dyadic scales, $k = 4$; (d) enhanced by scale variable edge stretching at 6 dyadic scales, $k_1 = 2$, $k_2 = k_3 = ... = k_6 = 4$. Histograms of the original and enhanced images are shown in Fig. 2.

(c) (d)

Figure 2: Histograms of the original and enhanced images in Fig. 1. (a) The histogram of the original low-contrast image in Fig. 1(a); (b) the equalized histogram; (c) the histogram of the image enhanced by constant multiscale edge stretching; (d) the histogram of the image enhanced by scale variable edge stretching.

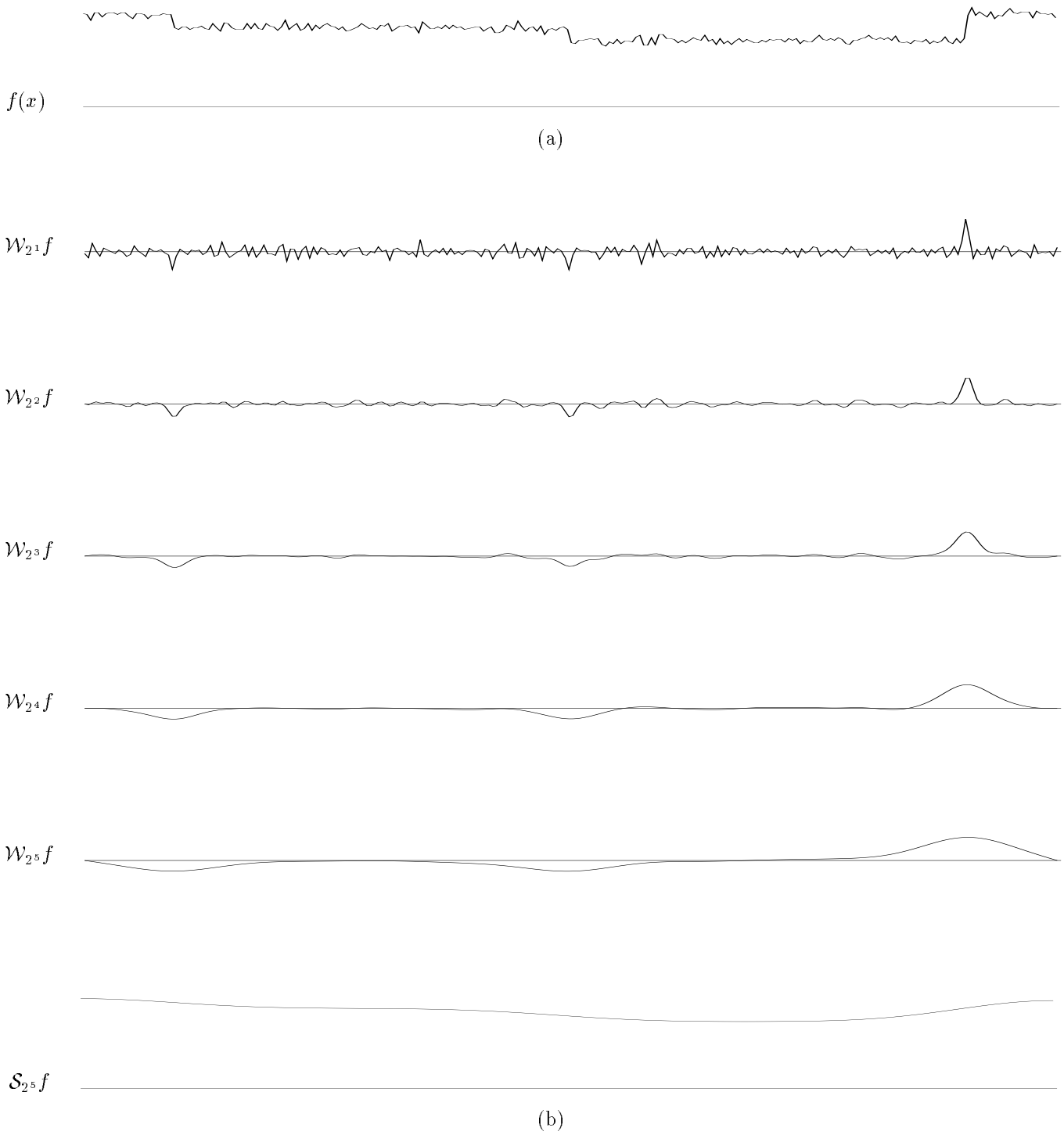

Figure 3: A line profile across the low-contrast cube image and the wavelet transform of the line profile. (a) Row #128 across the low-contrast cube image in Fig. 1(a); (b) The discrete wavelet transform of the line profile at 5 dyadic scales, which generates multiscale gradients.

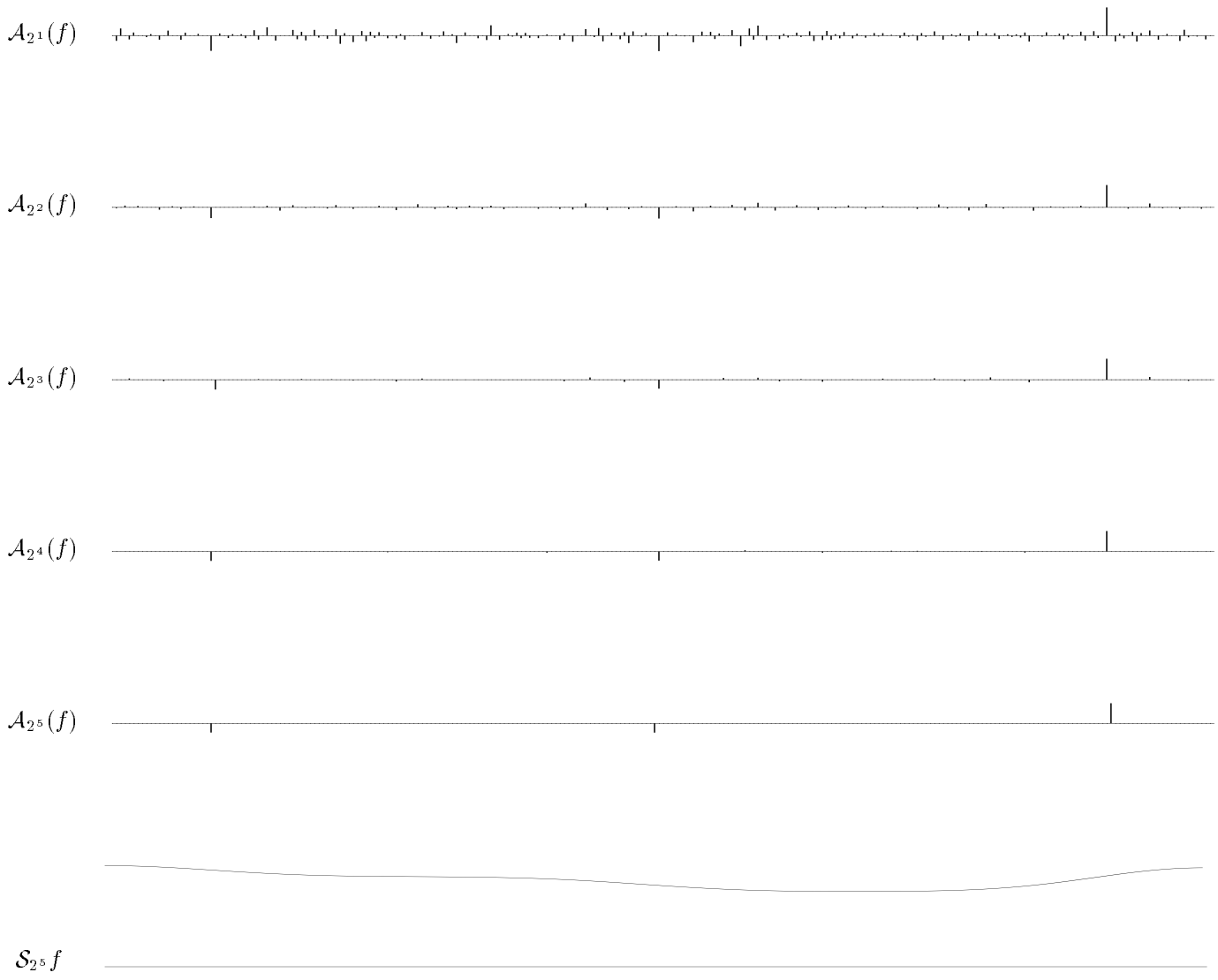

Figure 4: The multiscale edge representation of the line profile in Fig. 3(a). The representation set contains the positions, gradient magnitudes, and signs of multiscale edges, plus the coarsest approximation of the line profile at scale 2^5.

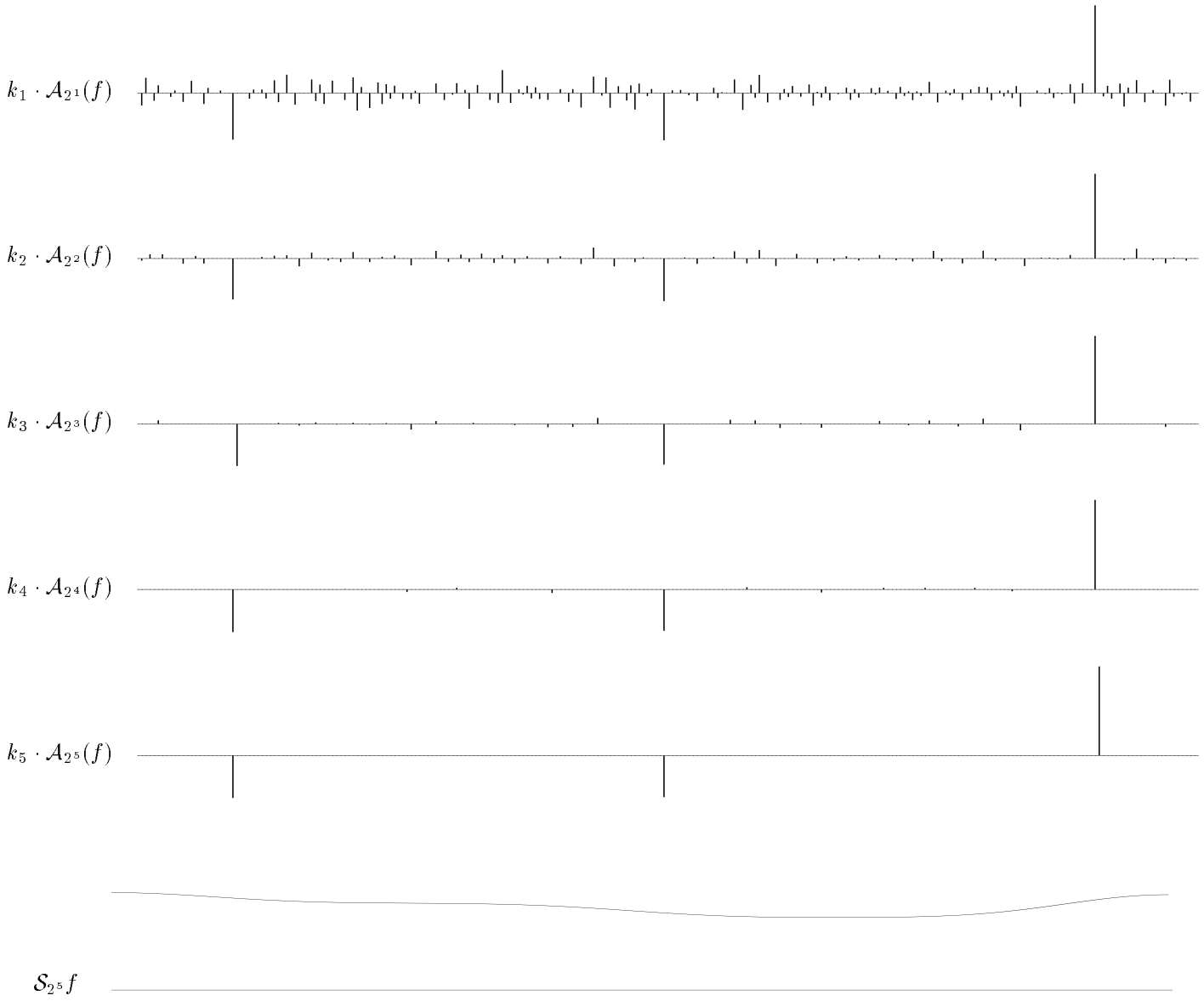

Figure 5: Linear stretching of multiscale edges. In this case, the stretching factors are: $k_1 = 2$, $k_2 = k_3 = k_4 = k_5 = 4$.

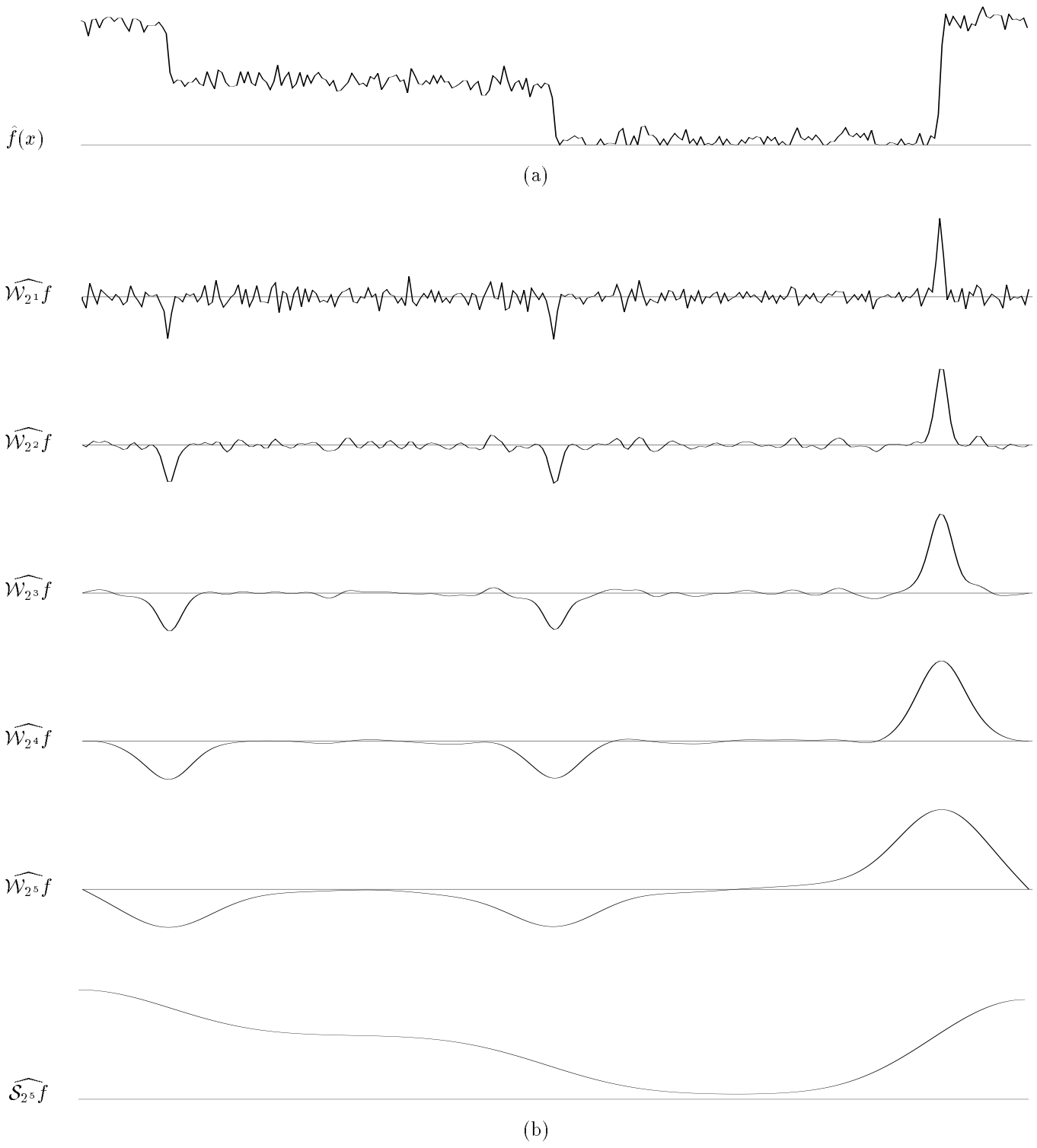

Figure 6: Reconstruction of a contrast-enhanced line profile. (a) Reconstructed by an inverse wavelet transform of (b); (b) reconstructed from Fig. 5 by an algorithm developed by Mallat and Zhong.

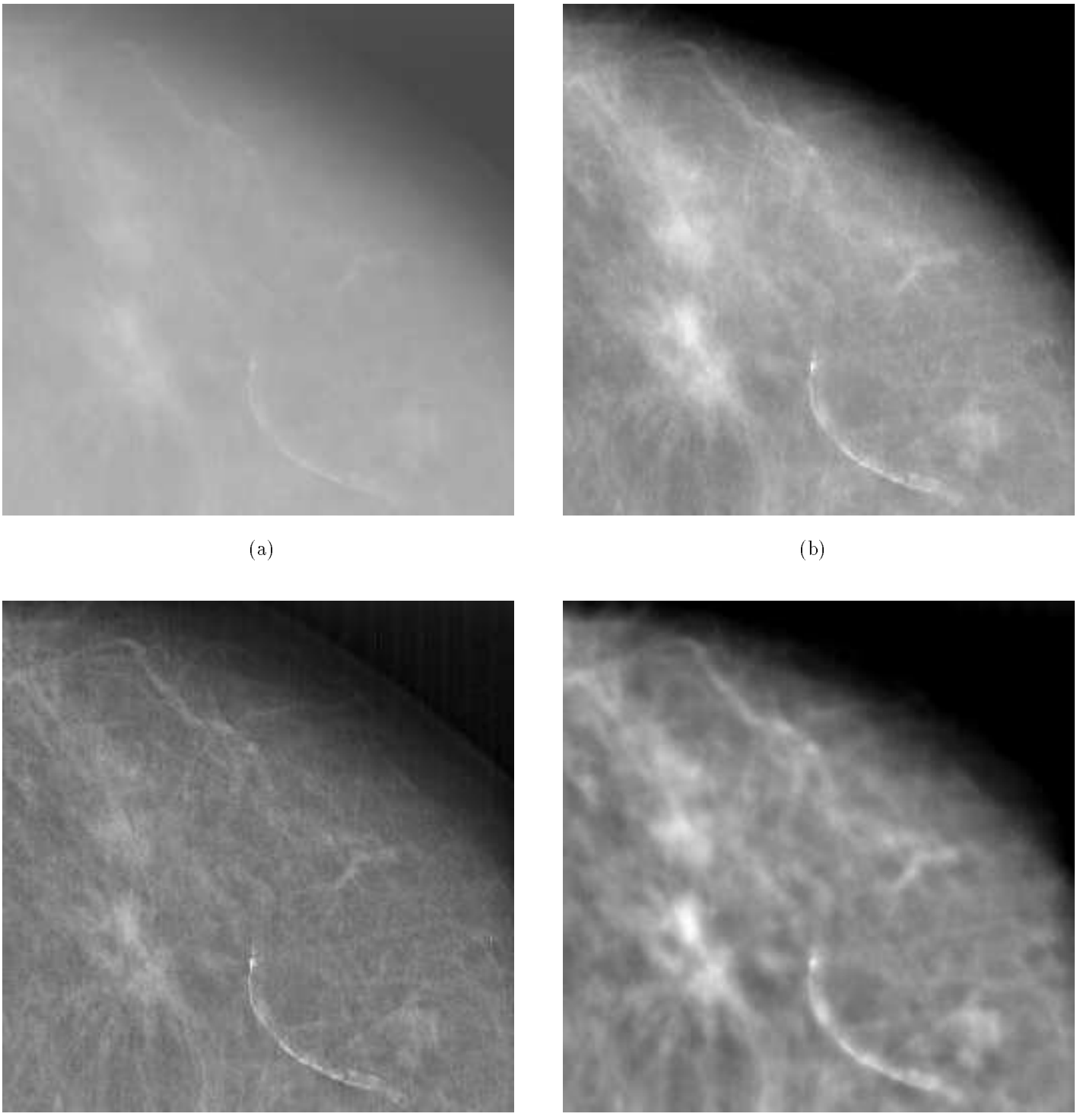

(a) (b)

(c) (d)

Figure 7: Enhancement of a mammographic image. (a) A portion of a digitized X-ray mammogram; (b) enhanced by constant multiscale edge stretching at 5 dyadic scales, $k = 5$; (c) enhanced by scale variable edge stretching at 5 dyadic scales, $k_1 = 5$, $k_2 = 4$, $k_3 = 3$, $k_4 = 2$, $k_5 = 1$; (d) enhanced by scale variable edge stretching at 5 dyadic scales, $k_1 = 2$, $k_2 = 6$, $k_3 = 12$, $k_4 = 6$, $k_5 = 2$.

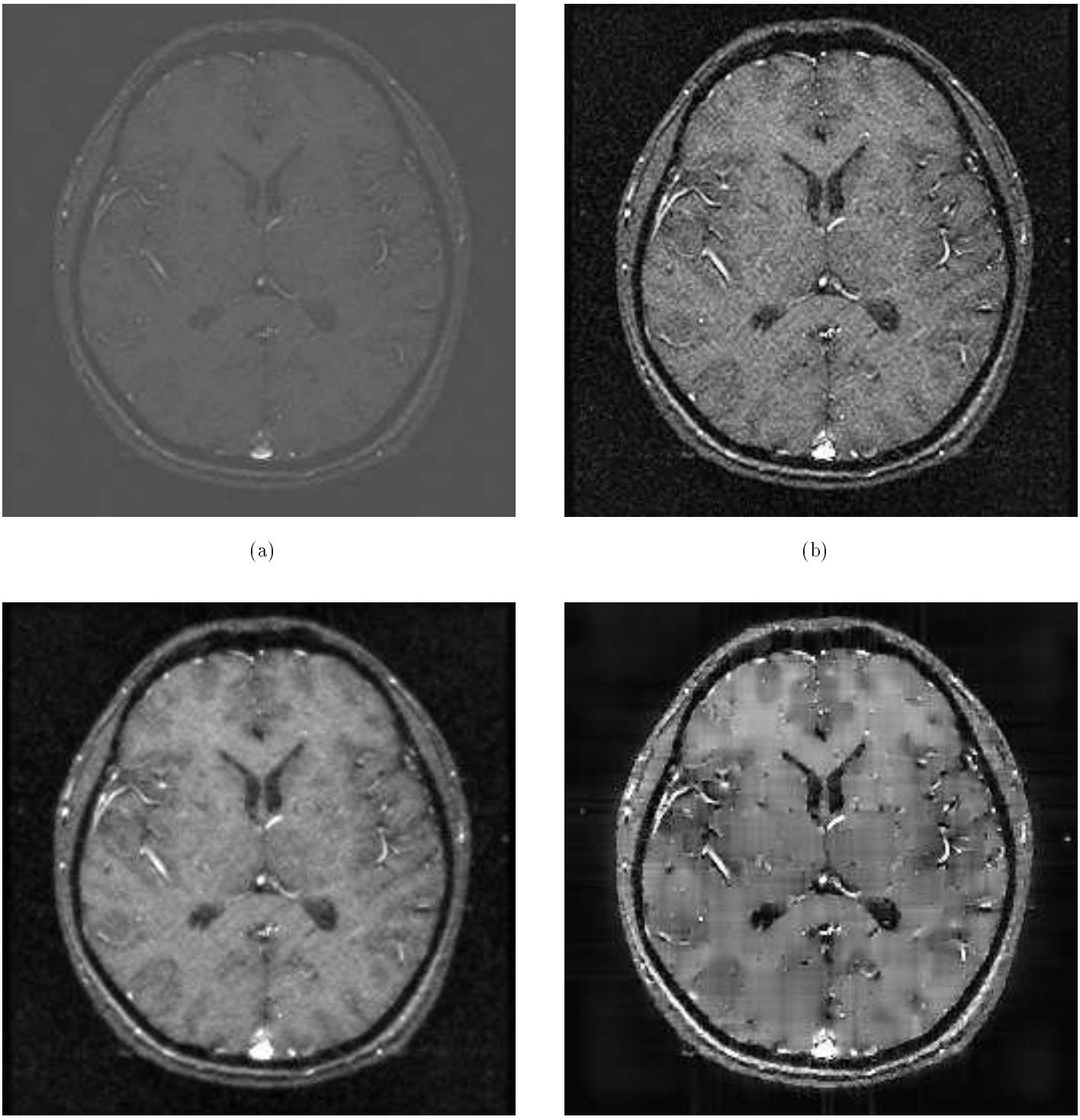

(a) (b)

(c) (d)

Figure 8: Enhancement of an MR image. (a) A low-contrast MR image of a human head; (b) enhanced by constant multiscale edge stretching at 5 dyadic scales, $k = 5$; (c) enhanced by scale variable edge stretching at 5 dyadic scales, $k_1 = 2$, $k_2 = k_3 = k_4 = k_5 = 5$; (d) enhanced by constant multiscale edge stretching at 5 dyadic scales with prefiltering by a denoising algorithm, $k = 5$.

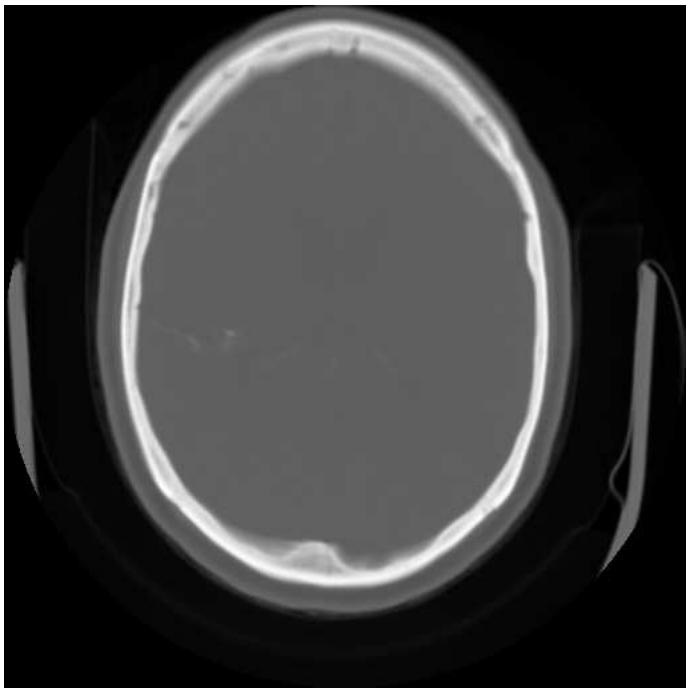

(a)

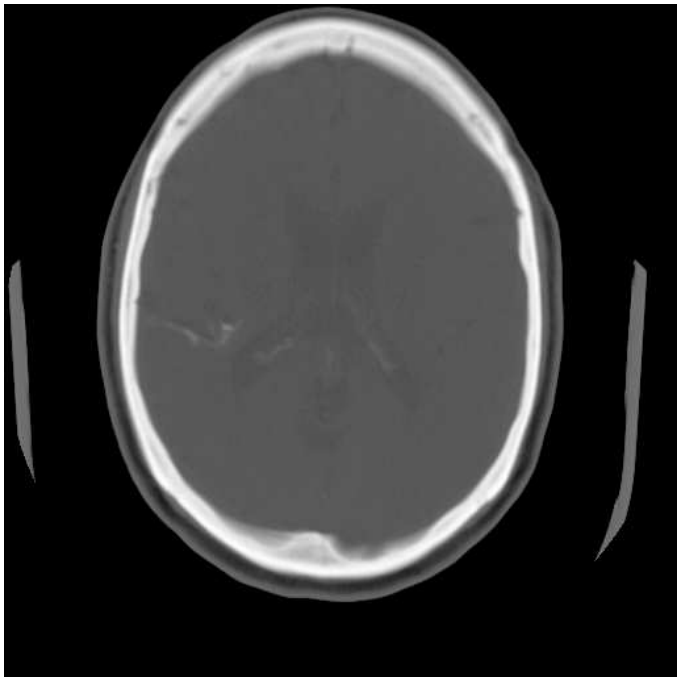

(b)

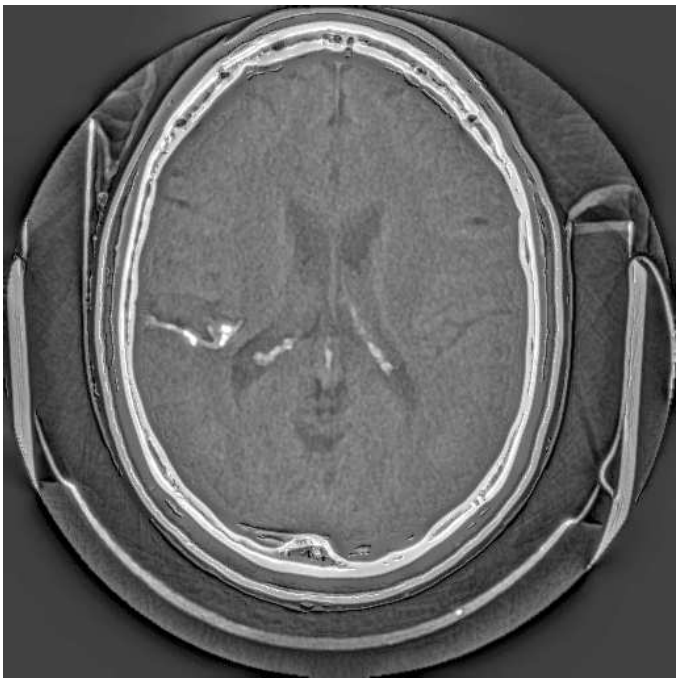

(c)

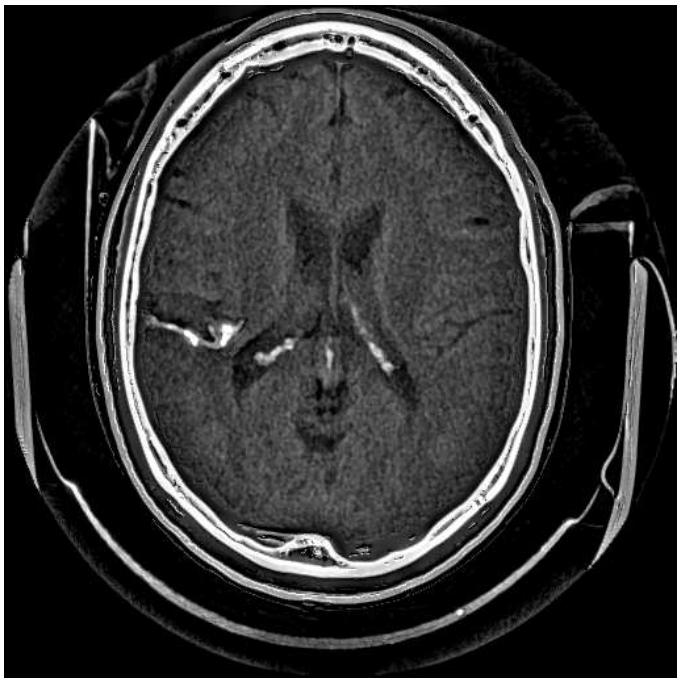

(d)

Figure 9: Enhancement of a CT image. (a) An X-ray CT image of a human head; (b) enhanced by constant multiscale edge stretching at 5 dyadic scales; (c) enhanced by gradient-dependent multiscale edge stretching and requantized without clipping; (d) enhanced by gradient-dependent multiscale edge stretching and requantized with clipping at both high and low ends of the intensity values.

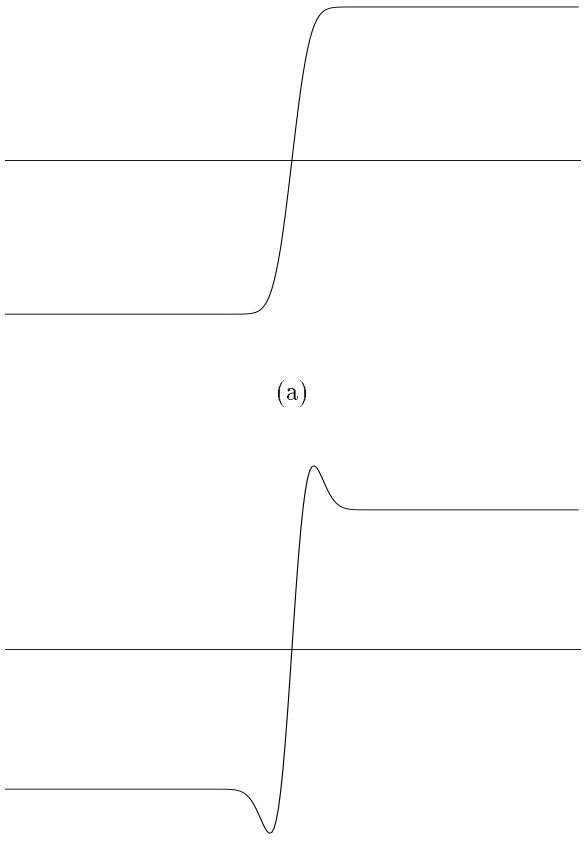

Figure 10: The effect of unsharp masking. (a) A profile of a smoothed step edge; (b) the result of unsharp masking by a Laplacian-of-Gaussian operator.